Available online at www.sciencedirect.com
ScienceDirect
Organic Electronics 9 (2008) 310–316
Organic Electronics
www.elsevier.com/locate/orgel

High-performance solution-processed polymer space-charge-limited transistor

Yu-Chiang Chao [a], Hsin-Fei Meng [a,*], Sheng-Fu Horng [b], Chain-Shu Hsu [c]

[a] *Institute of Physics, National Chiao Tung University, Hsinchu 300, Taiwan, ROC*
[b] *Department of Electrical Engineering, National Tsing Hua University, Hsinchu 300, Taiwan, ROC*
[c] *The Department of Applied Chemistry, National Chiao Tung University, Hsinchu 300, Taiwan, ROC*

Received 19 July 2007; received in revised form 22 November 2007; accepted 27 November 2007
Available online 15 December 2007

Abstract

We demonstrate a polymer non-field-effect transistor in a vertical architecture with an Al grid embedded in a polymer sandwiched between another two electrodes. The Al grid containing high density of self-assembled submicron openings is fabricated by a non-lithography method. This device modulates the space-charge-limited current of a unipolar polymer diode with the Al grid. The operating voltage of the device is as low as 4 V, the on/off ratio is higher than one hundred, and the current gain is 10^4. The current density is higher than 1 mA/cm^2.

PACS: 85.30.De; 73.61.Ph

Keywords: Space-charge-limited current; Vertical transistor

1. Introduction

An explosion of interests in flexible electronics made from organic semiconductors gave rise to extensive research on polymer light-emitting diodes (PLED), polymer field-effect transistors (FET), polymer chemical sensors and polymer solar cells. One of the key components of the flexible electronics is the polymer FET, a horizontal device with source and drain electrodes in the same plane. Its operating voltage usually exceeds 20 V due to low carrier mobility. The characteristics of polymer FETs can be strengthened by increasing the mobility [1], utilizing a self-assemble monolayer as gate dielectrics [2] and reducing the channel lengths to the submicron [3]. Horizontal organic FETs with submicron channel lengths made by electron-beam lithography [4], nanoimprint lithography [5] and soft contact lamination [6] have been demonstrated. Vertical organic FETs, whose channel length was determined by the thickness of an insulating layer between source and drain, have been made by solid-state embossing [7], excimer laser [8] and photolithography [9]. However, the inherently low mobility as well as the incompatibility between conventional submicron lithography and organic

* Corresponding author. Tel.: +886 3 5731955.
E-mail address: meng@mail.nctu.edu.tw (H.-F. Meng).

1566-1199/$ - see front matter © 2007 Elsevier B.V. All rights reserved.
doi:10.1016/j.orgel.2007.11.012

materials pose great limitation on the device performance and the fabrication process for polymer FET. The unique advantages of organic materials such as low-cost and large-area solution process are so far not fully explored for high-performance FET. Vertical non-field-effect transistors with multilayer structures give another route to circumvent the limits of both horizontal and vertical field-effect transistors. In vertical non-field-effect transistors, the channel length can be easily defined by the total thickness of the organic layers, and the current is modulated by a conductive layer embedded in the organic materials. Various device operating principles were proposed with different types of conductive layers such as a thin metal film [10–12], a strip-type metal film [13,14], a mesh gate electrode [15–17], and a porous conducting polymer network [18]. The remaining problems are the low current density, low on/off ratio as well as the complex fabrication process. One promising direction is to turn a vacuum tube triode into a solid-state device with current limited by the space-charge-limited current (SCLC), following the initial attempt of Shockley [19] in 1952. Vacuum tube triode is a three terminal device which consists of cathode and anode for electron emission and collection as well as the grid for current modulation. The on and off state of the vacuum tube triode is determined by whether the emitted electrons encounter a large energy barrier between cathode and anode or not. Recently, we demonstrated the polymer space-charge-limited transistor (SCLT) which functions similar to the vacuum tube triode [20]. A metal with random openings made by non-lithographic method is used as the grid. The output current density is however only about 0.01 mA/cm^2 due to the difficulty in realizing high opening density. In this work we solve that difficulty and the current density is significantly raised by two orders of magnitudes to as high as 1 mA/cm^2, which is nearly enough to drive a high-efficiency phosphorescent organic LED with the same area.

The schematic device structure and the energy band diagram are shown in Fig. 1. Poly(3,4-ethylenedioxythiophene):poly(styrenesulfonate) (PEDOT:PSS), with a work function of 5.2 eV, was used as an Ohmic contact for hole injection into the highest occupied molecular orbital (HOMO) of poly(3-hexylthiophene) (P3HT) at 5.1 eV. As the transistor is on, the injected holes can pass through the openings on Al grid and collected by Al collector electrode. The Al grid, functions similarly to the grid in vacuum tube triode, is an Al film with a high density of random submicron openings. The polystyrene spheres are used as the shadow mask for Al deposition to form Al grid, and the openings are formed at the positions of the spheres. The current density is proportional to the opening density. We form Al grid with high opening density using controlled assembly of polystyrene spheres on hydrophobic polymer surface, resulting a much higher current density.

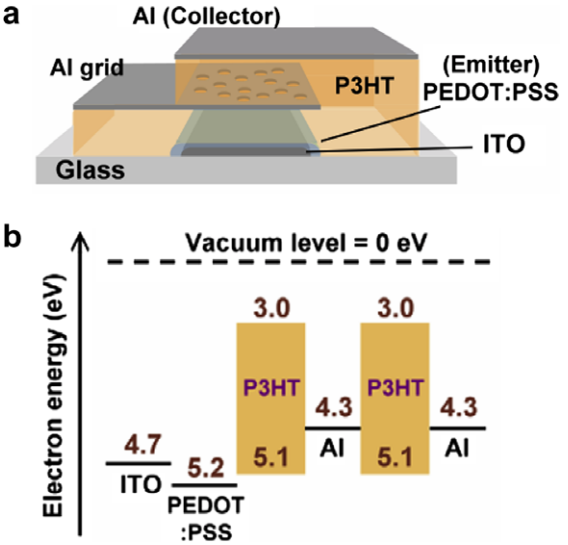

Fig. 1. (a) Device structure of polymer SCLT with an Al grid with random submicron openings. (b) Energy band diagram of polymer SCLT. The energies are indicated in eV. The solid line is the Fermi level of Al and PEDOT:PSS. The LUMO and HOMO energy for P3HT are 3 and 5.1 eV. The thickness between PEDOT and Al grid is 200 Å, and 300 Å between grid and Al collector.

2. Experimental

The device is fabricated on a cleaned indium–tin-oxide (ITO) glass substrate with a layer of 400 Å PEDOT:PSS. After baking in glove box at 200 °C for 10 min, P3HT is spin coated from chlorobenzene solution (1.5 wt.%) on the PEDOT:PSS layer and anneal at 200 °C for 10 min. A spin rinsing with xylene is used to remove the remaining soluble part of P3HT, even though the P3HT annealing condition has been chosen to have an almost fixed thickness after spin rinsing. After depositing the polystyrene spheres on the P3HT surface with the method described in the next section, the 150 Å Al grid is evaporated. After removing the polystyrene spheres by an adhesive tape, a layer of 300 Å P3HT is spin

coated from xylene solution (1.3 wt.%). An Al film of 300 Å is finally deposited to complete the device. The device active area is 1 mm^2.

A variety of self-assembly strategies of polystyrene spheres have been developed for hydrophilic surface to form two dimensional colloidal arrays [16,17,21,22]. A major problem to achieve a high density of separated colloid spheres is the hydrostatic attraction among the spheres. Fujimoto et al. [16] rinsed the samples in 98 °C water to avoid the sphere aggregation on the hydrophilic glass substrate. However, for the hydrophobic surface of the polymer like P3HT, modifications of these strategies are necessary. We use ethanol to dilute the polystyrene spheres (Sigma–Aldrich) for decreasing the contact angle since its alkyl group improves the adhesion between polymer and polystyrene ethanol solution. The polystyrene spheres are absorbed on the P3HT film surface by submerging the film in a polystyrene spheres ethanol solution for tens of seconds. The key procedure in the fabrication is that the substrate is then transferred to a beaker with boiling isopropanol solution for 10 s. Similar to the method of Fujimoto et al. [16], the substrate is finally blown dry immediately in a unidirectional nitrogen flow. After the Al deposition as Al grid, the polystyrene spheres are removed by an adhesive tape (Scotch, 3 M) without damage to the metal. The atomic force microscopy (AFM, Digital Instruments D3100) images of the Al grid with 1000 Å and 2000 Å opening diameter are shown in Fig. 2. The boiling isopropanol treatment is a critical step to achieve a high density yet separated array of holes, required for vacuum tube triode as well as SCLT. When the substrate is submerged in polystyrene solution, the charged polystyrene spheres are absorbed on the P3HT surface without aggregation due to the electrostatic repulsion force. Without the boiling isopropanol treatment, the polystyrene spheres are easy to aggregate during the drying process and cause unwanted non-uniform and connected distribution (Fig. 2f). This may be attributed to the capillary force which pulls spheres into aggregates before the spheres are immobile when the solvent is vaporized. The importance of the boiling isopropanol treatment is presumed to increase the evaporation rate of the solvent during the nitrogen blow dry such that the spheres do not have enough time to move to one another and form aggregate during evaporation. Another possible advantage of the boiling solvent is that it partially melts the spheres and glues the spheres on the surface. With the boiling isopropanol treatment, the opening density on the Al grid indeed increases dramatically, and the openings remain separated. The opening density on the Al grid increases with increasing solution concentration and submerging time (Fig. 2a–d). However, the amount of openings with irregular shape and size also increases (Fig. 2e). This may be due to the high capillary force between spheres with very short distance when the sphere density is high, or due to the unabsorbed spheres in the fluid over the film. One way to remove these unabsorbed spheres is gently rinsing the surface with ethanol or isopropanol before boiling isopropanol treatment. In spite of some occurrence of the unwanted irregular openings, the condition to prepare Al grid with maximum opening density with minimum unwanted openings can be found by tuning the solution concentration and submerging time. The benefit of this method is the possibility to process large-areas in a short processing time without photolithography.

3. Results and discussions

The characteristics of polymer SCLT with opening diameters of 1000 Å and 2000 Å on Al grid are shown in Fig. 3a and c. First note there is one major difference on the grid current I_G between vacuum tube and SCLT. The grid electrode in vacuum tube is not heated so the possibility for the electrons to enter the vacuum by thermal excitation from the grid is practically zero. There is therefore no need to consider the current gain which is defined as the ratio between the collector current and grid current. However in SCLT the carriers in the Al grid are blocked only by the Schottky barrier of 0.8 eV between Al and P3HT. In fact the grid current is the reverse current of the Al/P3HT Schottly diode which is small but not zero. The current gain is therefore an important value to be maximized. As shown in Fig. 3b and d, the grid current I_G of our devices is in the order of 10^{-9} A which is much smaller than I_C. The current gain I_C/I_G is as large as 10^4. For fixed collector voltage the collector current I_C is modulated by the grid voltage V_G. The emitter is the common ground. V_G is limited to be no more negative than −1 V otherwise the emitter-grid diode would turn on and cause large I_G. The positive V_G is used to introduce energy barrier for holes at the openings, and the off current can be reduced by increasing V_G until a large leakage current between the grid and collector occurs. The

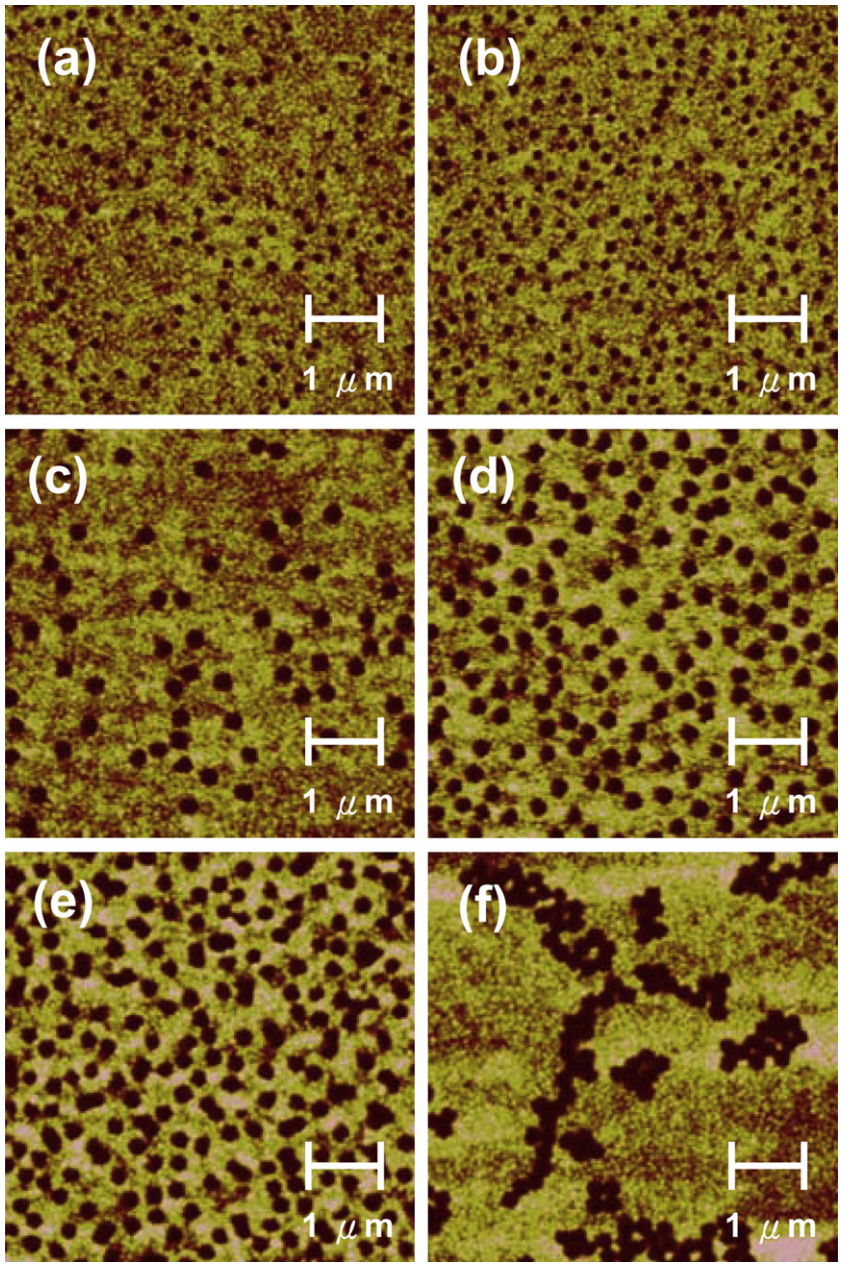

Fig. 2. Al grid with opening diameter of 1000 Å prepared by submerging the substrate in (a) 0.05 wt.%, and (b) 0.1 wt.% polystyrene solutions for 20 s with the boiling isopropanol treatment. Al grid with opening diameter of 2000 Å prepared by submerging the substrate in (c) 0.08 wt.%, (d) 0.24 wt.% and (e) 0.4 wt.% polystyrene solutions for 40 s with the boiling isopropanol treatment. (f) Same condition in (e) but without the boiling isopropanol treatment. The height scale is 30 nm for each image and the dimensions of the image is $5 \times 5\ \mu m^2$.

on/off ratio of I_C is 123 and 116 at $V_C = -4$ V, respectively, for transistors with opening diameters of 1000 Å and 2000 Å on Al grid. The highest I_C output is 1.14×10^{-5} A in Fig. 3c, corresponding to 1.14 mA/cm^2 for active area of 1 mm^2. Note the total output current can be easily scaled up by using a larger area. In order to look for the signature of SCLC, the device characteristics in double logarithmic scale with fixed V_G are shown in the inset of Fig. 3a and c. Three regions belonging to ohmic, trap filling and SCLC can be distinguished [23]. The slope of $\log I - \log V$ is equal to 1 for ohmic conduction, while the slope is equal to 2 for SCLC. The dashed lines with slope equal to 1 and 2 are

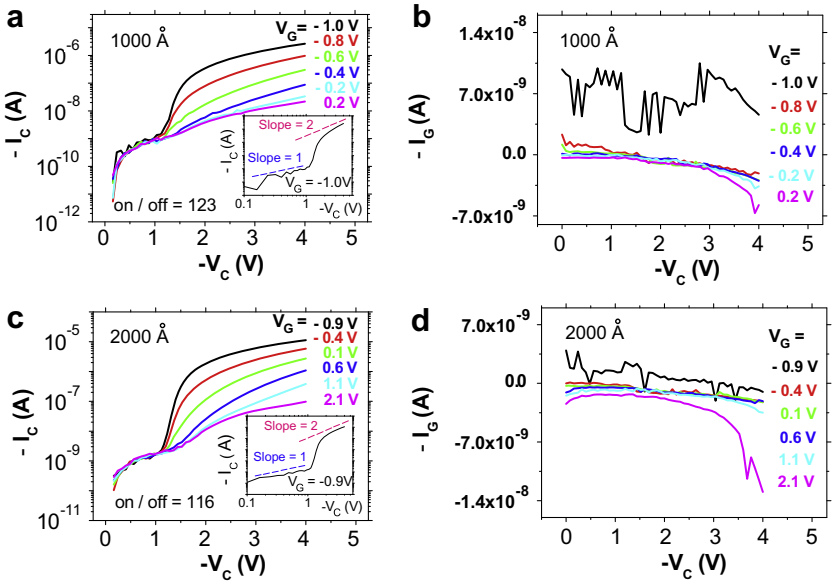

Fig. 3. The electric characteristics of the polymer SCLT with various grid voltages applied. The ITO electrode is commonly grounded and the Al collector is negatively biased at V_C with respect to ITO. The negative collector current I_C means the holes are collected by the Al collector and flows out from the transistor. The gate current I_G is no more than a few nA for all measurements. (a) The collector current as a function of the collector voltage. During the fabrication procedure, the 0.05 wt.% solution of polystyrene spheres with diameters of 1000 Å is used. The submerging time is 20 s. The inset shows the characteristics in double logarithmic of the device with V_G equal to −1 V. (b) The grid current as a function of the collector voltage of the transistor with same fabrication procedure described in (a). (c) The collector current as a function of the collector voltage. During the fabrication procedure, the 0.08 wt.% solution of polystyrene spheres with diameters of 2000 Å is used. The submerging time is 40 s. The inset shows the characteristics in double logarithmic of the device with V_G equal to −0.9 V. (d) The grid current as a function of the collector voltage of the transistor with same fabrication procedure described in (c).

drawn in the inset of Fig. 3a and c for indication. Indeed, the current follows the SCLC once the barrier at the opening is suppressed by a negative enough V_C. At low voltage there is always a small ohmic current. The polymer diode has a turn-on voltage where the current switches from a small leakage ohmic current into a quadratic SCLC current. The turn-on voltage is determined by both the level of the leakage and the difference between the work functions of the cathode and anode. For our diode it is about 1 V as shown in Fig. 3.

The operation mechanism of the polymer SCLT can be understood as the quadratic space-charge-limited current between the emitter and the opening modulated by the grid potential. As in vacuum tube, the potential at the center of the opening is a linear combination of grid and collector potential $\lambda V_G + V_C$, the factor λ depends on the device geometry and increases with the ratio between the opening diameter and the grid-collector distance. The SCLC between the emitter and the opening is therefore approximately $C\,\varepsilon\mu\,(\lambda V_G + V_C)^2/L^3$, where ε is the polymer dielectric constant and L is the emitter-grid distance. If the potential across the opening were uniform, the factor C would be the standard SCLC value of 9/8. The overall effect of non-uniform potential in our case can be absorbed into a numerical factor C. Because of the higher electric field the space between the grid and the collector does not limit the collector current so the emitter-opening current given above is actually the output current.

The above analysis is based on the assumption that all the space charge and potential profiles are determined by the injected carriers instead of background doping. The active semiconductor P3HT is an intrinsic semiconductor without intentional doping. It is well known the main source of unintentional doping of P3HT is oxygen. The samples are fabricated in our glove box with oxygen level below 1 ppm. There are reports on the doping level of P3HT around 10^{15} cm^{-3} without particular attention on oxygen doping [24]. The sample fabrication process is carefully controlled to minimize the oxygen and water contamination. The water and oxygen level inside the glove box are both below 1 ppm. Dehydrated ethanol (≤0.2% water, Riedel-de-Haën)

is used for the polystyrene sphere deposition. The vacuum in the grid evaporation chamber is 10^{-7} torr, so most of the adsorbed oxygen molecules during ethanol immersion are expected to be removed by the high vacuum. Moreover the sample is annealed at 200 °C in vacuum after the spin coating of the second P3HT film. It is known that thermal treatment will significantly de-dope P3HT [25]. We therefore believe our doping level is below 10^{15} cm^{-3}. Even for 10^{15} cm^{-3} the calculated Debye–Huckel screening length is 700 Å which is larger than the total thickness of the SCLT. The electric field provided by the collector voltage is therefore not screened. The quadratic I_C–V_C relation indicates that the space charge is dominated by the injection carrier. This is also an evidence that the doping is not important for the device operation here.

The grid control of the current can be further illustrated by looking at the spatial distribution of the current across the opening. In general only some region near the center of the opening has negative potential for the holes to pass through. Near the edge the effect of the grid is so strong that a potential barrier forms despite of the negative potential of the collector. The current is therefore confined in an area controlled by the grid potential. As the transistor is in the on state, there is no barrier in all the area. The emitter–collector path through A position at the center and the path through B position near the edge of the opening have the potential profiles as the curves (x) and (y) in Fig. 4b, respectively. Assuming that the collector current is roughly a superposition of the currents of many small diodes given by the paths through different positions, the small diodes at position A contributing to a high current (A^{ON}) and those at position B are just about to be turned on (B^{ON}), as indicated in Fig. 4c. On the other hand as the device is in the off state, the grid potential is positive and there is a potential barrier at the B position as the curve (z) in Fig. 4b, and the small diodes there is reverse biased (B^{OFF}). As for A position, if it also has the potential profile like curve (z) in Fig. 4b, the off current comes from small diodes at position A will be small. However, if the potential profile is as the curve (y), there will be an undesirable leakage current from the barely-on small diode at A (A^{OFF}). Theoretically an even more positive grid potential can always drive it into

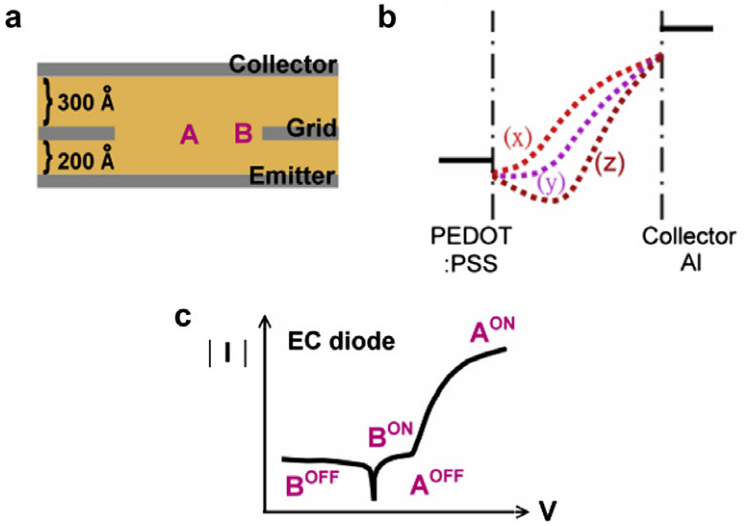

Fig. 4. (a) The device structure near one opening of polymer SCLT. Position A is at the center of the opening, while position B is near the grid. (b) The potential profile along the emitter–collector path through the opening when V_C is fixed at a negative value. (x), (y), (z) are the potential profile along the path for various conditions. Curve (x) is a potential profile without energy barrier for hole as in the case of a simple emitter–collector diode without the grid. Curve (z) is a potential profile with energy barrier for hole for a positive enough grid potential V_G. The barrier for hole diminishes while V_G drops from positive to negative as indicated by (y). Different position in the opening has different potential profile, which result from different $\lambda V_G + V_C$. (c) The schematic current–voltage curve of EC diode with the structure ITO/PEDOT/P3HT/Al. There is a turn-on voltage for the forward bias direction. The path through position A in on or off state are denote as A^{ON} or A^{OFF} in the diode IV curve. The double-sided arrow means off-state could be either reverse bias or small forward bias before turn-on. The state of the path through B is also shown. Because of the proximity to the positive biased grid B path can never be fully turned on as A.

curve (z), but in practice breakdown of the grid/polymer Schottky junction may happen first.

4. Conclusion

In summary, we demonstrate the vertical polymer space-charge-limited transistor with high current density, high on/off ratio, high current gain, and low operation voltage. A non-lithography method is introduced for the desired high opening density on the metal grid embedded in the polymer. This non-field-effect device opens a new possibility for high-performance organic electronics with easy large-area solution process and vertical integration with organic light-emitting diodes without demanding a very high carrier mobility.

Acknowledgement

This work is supported by the National Science Council of the Republic of China under Contract No. NSC96-2112-M-009-036.

References

[1] I. Mcculloch, M. Heeney, C. Bailey, K. Genevicius, I. Macdonald, M. Shkunov, D. Sparrowe, S. Tierney, R. Wagner, W. Zhang, M.L. Chabinyc, R.J. Kline, M.D. Mcgehee, M.F. Toney, Nature Mater. 5 (2006) 328.
[2] M. Halik, H. Klauk, U. Zschieschang, G. Schmid, C. Dehm, M. Schütz, S. Maisch, F. Effenberger, M. Brunnbauer, F. Stellacci, Nature 431 (2004) 963.
[3] J.Z. Wang, Z.H. Zheng, H.W. Li, W.T.S. Huck, H. Sirringhaus, Nature Mater. 3 (2004) 171.
[4] Y. Zhang, J.R. Petta, S. Ambily, Y. Shen, D.C. Ralph, G.G. Malliaras, Adv. Mater. 15 (2003) 1632.
[5] M.D. Austin, S.Y. Chou, Appl. Phys. Lett. 81 (2002) 4431.
[6] J. Zaumseil, T. Someya, Z. Bao, Y.-L. Loo, R. Cirelli, J.A. Rogers, Appl. Phys. Lett. 82 (2003) 793.
[7] N. Stutzmann, R.H. Friend, H. Sirringhaus, Science 299 (2003) 1881.
[8] R. Parashkov, E. Becker, G. Ginev, T. Riedl, M. Brandes, H.-H. Johannes, W. Kowalsky, Appl. Phys. Lett. 85 (2004) 5751.
[9] R. Parashkov, E. Becker, S. Hartmann, G. Ginev, D. Schneider, H. Krautwald, T. Dobbertin, D. Metzdorf, F. Brunetti, C. Schildknecht, A. Kammoun, M. Brandes, T. Riedl, H.-H. Johannes, W. Kowalsky, Appl. Phys. Lett. 82 (2003) 4579.
[10] M.S. Meruvia, I.A. Hümmelgen, M.L. Sartorelli, A.A. Pasa, W. Schwarzacher, Appl. Phys. Lett. 84 (2004) 3978.
[11] Y.C. Chao, S.L. Yang, H.F. Meng, S.F. Horng, Appl. Phys. Lett. 87 (2005) 253508.
[12] K.I. Nakayama, S.Y. Fujimoto, M. Yokoyama, Appl. Phys. Lett. 88 (2006) 153512.
[13] K. Kudo, D.X. Wang, M. Iizuka, S. Kuniyoshi, K. Tanaka, Thin Solid Films 331 (1998) 51.
[14] Y. Watanabe, K. Kudo, Appl. Phys. Lett. 83 (2005) 223505.
[15] N. Hirashima, N. Ohashi, M. Nakamura, K. Kudo, IPAP Conf. Series 6 (2005) 158.
[16] K. Fujimoto, T. Hiroi, M. Nakamura, e-J. Sci. Nanotech. 3 (2005) 327.
[17] K. Fujimoto, T. Hiroi, K. Kudo, M. Nakamura, Adv. Mater. 19 (2007) 525.
[18] Y. Yang, A.J. Heeger, Nature 372 (1994) 344.
[19] W. Shockley, Proc. IRE 40 (1952) 1289.
[20] Y.C. Chao, H.F. Meng, S.F. Horng, Appl. Phys. Lett. 88 (2006) 223510.
[21] Y. Xia, B. Gates, Y. Yin, Y. Lu, Adv. Mater. 12 (2000) 693.
[22] C. Werdinius, L. Österlund, B. Kasemo, Langmuir 19 (2003) 458.
[23] Z. Chiguvare, V. Dyakonov, Phys. Rev. B 70 (2004) 235207.
[24] E.J. Meijer, A.V.G. Mangnus, C.M. Hart, D.M. de Leeuw, T.M. Klapwijk, Appl. Phys. Lett. 78 (2001) 3902.
[25] B. Mattis, P. Chang, V. Subramanian, Synth. Met. 156 (2006) 1241.